Research Article

Reham Saleh, Samar Elsanabary, and Abla Elmegharbel*

Thermo-elastic analysis of curved beam made of functionally graded material with variable parameters

https://doi.org/10.1515/cls-2025-0037
received December 08, 2024; accepted August 09, 2025

Abstract: This work presents an analytical derivation for the stress and deformation formulations under combined mechanical and thermal loading in rectangular functionally graded curved beams. The mechanical load consists of a double couple, while the thermal load corresponds to a steady-state temperature distribution. Using Timoshenko beam theory and thermo-elastic theory, the governing equations incorporate an exponential material gradient in the radial direction, assuming a constant Poisson's ratio. The Mathematica software was utilized to evaluate the stress and deformation formulations for the thermo-mechanical analysis. Meanwhile, Matlab software was used to perform the results. The results of normalized stresses (including radial, tangential, and von Mises components) and deformations are presented at different variations of temperatures for two different materials that are plotted. The results for the two considered FGM materials, Aluminum/steel and Ti-6Al-4V/ZrO_2 are compared, demonstrating lower stresses for Ti-6Al-4V/ZrO_2 under identical conditions. The study highlights the influence of temperature and material gradients that affect stress and deformation, with strong agreement between analytical results and finite element analysis (ANSYS simulations), validated through MATLAB plots.

Keywords: FGM curved beams, mechanical loads, thermal loads, FEA, ANSYS

*** Corresponding author: Abla Elmegharbel**, Production Engineering and Mechanical Design Department, Port-Said University, Port-Said, 42523, Egypt, e-mail: aelmegharbel@eng.psu.edu.eg
Reham Saleh: Production Engineering and Mechanical Design Department, Port-Said University, Port-Said, 42523, Egypt, e-mail: reham.saleh@eng.psu.edu.eg
Samar Elsanabary: Production Engineering and Mechanical Design Department, Port-Said University, Port-Said, 42523, Egypt, e-mail: samar.abaas@eng.psu.edu.eg

1 Introduction

In engineering applications, functionally graded materials (FGMs) are widely used in aerospace, automotive, biomedical, energy, and structural components. FGMs consist of a combination of two different constituents with distinct characteristics, resulting in an advanced material with properties that combine those of both constituent materials. The primary advantage of a gradually changing material property gradient in a specific direction is the mitigation of thermal and residual stresses in structural components, thereby preventing damage [1–3].

Curved beams are among the most essential structures in mechanical, architectural, and aerospace engineering. They efficiently transmit loads through their elements, enabling diverse industrial applications such as crankshafts, hooks, piston rings, and aerospace structural components [4].

Several studies have investigated the behavior of FGM curved beams under different conditions. Pei and Li [5] theoretically evaluated stresses and deformations in FGM curved beams using lower-order beam theory. He *et al.* [6] conducted a theoretical analysis of FGM curved beams under pure bending, accounting for the effect of grading parameters. The results demonstrated that the intermediate layer of the curved beam exhibited the highest magnitudes of tensile and compressive stresses.

Pydah and Sabale [7] developed an analytical solution for bi-directional FGM curved beams under various loads and grading parameters. The critical stresses and deformations were determined based on Euler–Bernoulli theory. Avhad and Sayyad [8] employed higher-order deformation theories to derive an analytical solution for FGM composite curved beams using the power-law mixture model. The results indicated that both deformation and axial stress increase with an increasing power index, while transverse stress decreases.

Zhang *et al.* [9] conducted an analysis of the FGM nano-curved beam using Timoshenko beam theory. The analytical

results demonstrated that the grading index significantly influences the deformation behavior of the curved beam. These findings were validated against both Euler–Bernoulli theory and previous analytical derivations for FGM curved beams. Belarbi *et al.* [10] developed a theoretical formulation for an advanced FGM curved beam, employing shear deformation and higher-order shear deformation theories to compute stresses and deformations while varying parameters, including the gradient index.

Karamanli *et al.* [11] proposed an analytical formulation for FGM curved beams using shear deformation theories to investigate deformation constraints under free vibration across different boundary conditions. A power-law function was applied to describe the material gradient, which varies in both radial and tangential directions.

Nikrad *et al.* [12] presented an analytical derivation for FGM curved beams under thermal loading, accounting for various porosity configurations, temperature distributions, curvature radii, and boundary conditions. Hu *et al.* [13] developed a novel multi-layered FGM model subjected to combined thermal and mechanical loads. Their analytical solution determined the deformation of multi-layered curved beams, incorporating the effects of undeformed curvature radius, thermo-mechanical coupling, and applied forces.

Tang *et al.* [14] investigated a circular FGM curved arch under combined thermal and buckling pressure effects. The stresses and deformations were evaluated by considering a variable power-law gradient index. Wan *et al.* [15] developed an analytical derivation for FGM curved beams using Timoshenko beam theory, incorporating key parameters: curvature radius, temperature variation, and material gradation. The results demonstrated that the curved beam's response was highly sensitive to these parameters.

Allam and Radwan [16] performed an analytical study of viscoelastic FGM curved nano-beams with multiple variable parameters. The power-law gradient theory was applied to analyze the beam's behavior under bending, buckling, and vibration. These theoretical results were validated against the analytical solution for FGM curved beams. Beg and Yasin [17] proposed an alternative analytical solution for deeply curved FGM beams under coupled thermal and dynamic loading, assuming a radial grading index variation. The results revealed that static, free, and forced vibration responses depended on the FGM layer count, thickness, and grading index. These findings were verified against 2D curved beam elasticity theory.

Pandey and Pradyumna [18] adopted higher-order layerwise beam assumptions to analyze curved FGM sandwich beams under thermal shock with variable parameters. Liang *et al.* [19] established an analytical model for a novel FGM curved beam-reinforced composite, utilizing Hamilton's principles and strain-displacement theory to characterize vibration-induced deformations.

Tornabene *et al.* [20] employed higher-order theory to develop a modified formulation for the thermo-electro-elastic analysis of laminated shell structures incorporating smart materials. Their analytical formulation was validated against finite element analysis (FEA), showing excellent agreement. Brischetto and Carrera [21] investigated thermal stress decoupling in multilayered composite shells using the Principle of Virtual Displacements and Carrera's Unified Formulation, with a linear temperature distribution assumed across the thickness. Shirdelan *et al.* [22] applied Hamilton's principle to derive an analytical solution for a five-layer doubly curved shell, examining the frequency response under various parameters. Civalek and Baltacıoglu [23] proposed two models of annular sector plates composed of FGM and laminated composites to analyze the frequency response using the first-order shear deformation theory.

A review of previous investigations reveals that few studies have adopted exponential functions to model FGM properties. Mahajan and Sharma [24] developed theoretical formulations for layered composite curved arches subjected to uniformly distributed loads. Their results demonstrated that static responses of sandwich and layered composite arches can be accurately predicted using exponential normal and shear deformation theories. Hussein *et al.* [25] evaluated the thermal conductivity ratio of FG fin subjected to grading boundary cooling and heating theoretically and numerically. Habib *et al.* [26] utilized an exponential function along the radial direction to analyze two FGM pressure vessels (SS304-SiC and TZM-SiC). The study considered combined internal pressure, time-dependent variations, and transient temperature distributions through the cylinder thickness. The results revealed that material gradation significantly affects stress distributions.

The novelty of this work lies in examining the coupled effects of grading properties, mechanical loading, and thermal loading on the stress and deformation behavior of FGM curved beams. The equilibrium equations, derived from thermoelastic theory, incorporate an exponential law to describe material property variations. The analytical solution yields radial, tangential, and von Mises stresses, along with deformation profiles, for two FGM material systems. Normalized stresses and deformations are presented as functions of normalized radius using MATLAB. Excellent agreement is observed between the analytical results and FEA performed with ANSYS.

2 Analytical formulations

2.1 Material gradient of FGM curved beam

FGMs, as advanced composites, consist of two distinct materials with continuously varying volume fractions across their geometry. The FGM curved beam considered in this study comprises two isotropic materials, with material properties described by an exponential function. Specifically, the modulus of elasticity E(r) is defined by the following exponential relationship:

$$E(r) = E_2 e^{\zeta\left(1-\frac{r}{R_2}\right)}, \tag{1}$$

where $E(r)$ is the position-dependent modulus of elasticity, r represents the radial coordinate, E_2 denotes the modulus at the outer surface (radius R_2), and ζ is the material grading parameter.

The effective material properties of the FGM curved beam, including Young's modulus, thermal expansion coefficient, thermal conductivity, and density, are determined using the mixture law. Accordingly, the material property gradient follows the relation:

$$P_{r_{\text{eff}}}(r) = P_{r_1}V_1(r) + P_{r_2}V_2(r), \tag{2}$$

where $P_{r_{\text{eff}}}(r)$ is defined as the curved beam's material properties (Young's modulus E, thermal coefficient α, thermal conductivity K, density ρ) as a function of r, where r is a variable radius that spans the curved beam's lower surface R_1 and upper surface R_2, where $R_1 \le r \le R_2$. P_{r_1}, and P_{r_2} are the material properties of material 1 and material 2 as a function of r, respectively. $V_1(r)$ and $V_2(r)$ are the volume fraction of material 1 and material 2 as a function of r, respectively.

The volume fraction is

$$V_2(r) = 1 - V_1(r), \tag{3}$$

$$E(r) = E_1V_1(r) + E_2V_2(r). \tag{4}$$

By substituting Eqs. (1) and (3) into Eq. (4),

$$V_1(r) = \frac{E_2 e^{\zeta\left(1-\frac{r}{R_2}\right)} - E_2}{E_1 - E_2}. \tag{5}$$

By substituting Eqs. (3) and (5) into the mixture law Eq. (2),

the result is shown in Eq. (6):

$$P_{r_{\text{eff}}}(r) = \frac{E_2 e^{\zeta\left(1-\frac{r}{R_2}\right)}(P_{r_1} - P_{r_2})}{E_1 - E_2} + \frac{P_{r_2}E_1 - P_{r_1}E_2}{E_1 - E_2}. \tag{6}$$

Assume

$$\beta_{\text{pr}} = \frac{E_2(P_{r_1} - P_{r_2})}{E_1 - E_2} \text{ and } \eta_{\text{pr}} = \frac{P_{r_2}E_1 - P_{r_1}E_2}{E_1 - E_2}$$

$$P_{r_{\text{eff}}}(r) = \beta_{\text{pr}} e^{\zeta\left(1-\frac{r}{R_2}\right)} + \eta_{\text{pr}}. \tag{7}$$

Eq. (7) governs the gradation of mechanical properties through the thickness of the curved beam. By substituting the thermal expansion coefficients of the constituent materials, the through-thickness variation of the thermal expansion coefficient is obtained as follows:

$$\alpha(r) = \beta_\alpha e^{\zeta\left(1-\frac{r}{R_2}\right)} + \eta_\alpha, \tag{8}$$

where β_α and η_α are the gradient parameters governing the thermal expansion coefficient variation in the FGM curved beam. These parameters are determined by the operating conditions. With the assumption of a constant Poisson's ratio, the material properties vary exclusively along the radial direction.

2.2 The basic equations

Figure 1 shows an FGM curved beam with a rectangular cross-section, where

- Inner radius: R_1
- Outer radius: R_2

The beam is subjected to combined mechanical and thermal loading, with a radially varying temperature distribution $T = T(r)$ following the assumption in the previous study [27]. Under plane stress conditions $\sigma_z = 0$, the analysis proceeds with the following considerations:

$$\sigma_{r_{r=a}} = 0, \quad \sigma_{r_{r=b}} = 0. \tag{9}$$

The radial displacement, according to Timoshenko's assumption, is

$$r = r_0, \theta = 0 \quad \text{and} \quad u(r_0, \theta = 0) = 0, \tag{10}$$

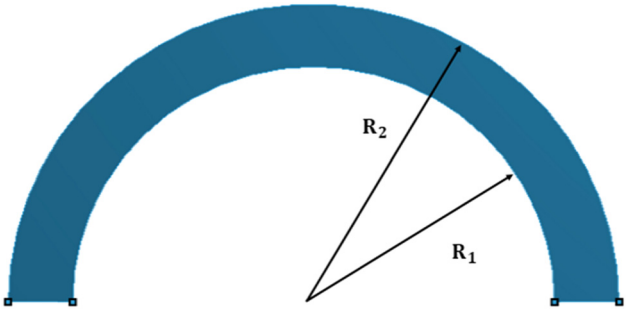

Figure 1: FGM curved beam geometry.

where r_0 is the radius of the FGM curved beam's initial, middle surface, where $r_0 = \frac{R_1 + R_2}{2}$, and u is the radial displacement.

According to the notation of Timoshenko [27], the strain displacement relations are as follows:

$$\varepsilon_r = \frac{du}{dr}, \tag{11}$$

$$\varepsilon_\theta = \frac{u}{r} + \frac{1\partial v}{r\partial\theta}, \tag{12}$$

where

- ε_r: Radial strain
- ε_θ: Tangential strain
- u: Radial displacement

Substituting the expression for u from Eq. (12) into Eq. (11) and integrating yield the compatibility condition:

$$\frac{\partial}{\partial r}(r\varepsilon_\theta) - \varepsilon_r = c_1. \tag{13}$$

The equilibrium equation is

$$\sigma_\theta = \frac{d}{dr}(r\sigma_r). \tag{14}$$

Assume the Poisson's ratio is constant.

The radial and tangential stresses can be expressed in terms of stress functions [28] as follows:

$$\sigma_r = \frac{F}{r}, \tag{15}$$

where F is the stress function

$$\sigma_\theta = \frac{dF}{dr}. \tag{16}$$

The radial and tangential deformation, respectively, are

$$u = \delta = r\varepsilon_\theta - c_1 r - c_2\cos\theta, \tag{17}$$

$$v = c_1 r\theta + c_2\sin\theta. \tag{18}$$

2.3 Thermoelasticity analytical solution

The FGM curved beam is assumed to exhibit linear thermoelastic behavior. Therefore, the constitutive relations derived from the generalized Hooke's law under thermal conditions are as follows:

$$\varepsilon_r = \frac{1}{E(r)}[\sigma_r - \nu\sigma_\theta] + \alpha(r)T, \tag{19}$$

$$\varepsilon_\theta = \frac{1}{E(r)}[\sigma_\theta - \nu\sigma_r] + \alpha(r)T. \tag{20}$$

By substituting Eqs. (1), (15), and (16) into Eqs. (19) and (20),

$$\varepsilon_r = \frac{1}{E_2 e^{\zeta\left(1-\frac{r}{R_2}\right)}}\left[\frac{F}{r} - \nu\frac{dF}{dr}\right] + \beta_\alpha e^{\zeta\left(1-\frac{r}{R_2}\right)}T + \eta_\alpha T, \tag{21}$$

$$\varepsilon_\theta = \frac{1}{E_2 e^{\zeta\left(1-\frac{r}{R_2}\right)}}\left[\frac{dF}{dr} - \nu\frac{F}{r}\right] + \beta_\alpha e^{\zeta\left(1-\frac{r}{R_2}\right)}T + \eta_\alpha T. \tag{22}$$

By substituting Eqs. (21) and (22) into Eq. (13), the resulting equation is

$$\begin{aligned}&\frac{r}{E_2 e^{\zeta\left(1-\frac{r}{R_2}\right)}}\frac{\partial^2 F}{\partial r^2} - \frac{\nu(r+1)}{E_2 e^{\zeta\left(1-\frac{r}{R_2}\right)}}\frac{dF}{dr} - \frac{1}{E_2 e^{\zeta\left(1-\frac{r}{R_2}\right)}}\frac{F}{r}\\ &+ \left(r\beta_\alpha e^{\zeta\left(1-\frac{r}{R_2}\right)} + \eta_\alpha\right)T' - \left(\beta_\alpha e^{\zeta\left(1-\frac{r}{R_2}\right)} + \eta_\alpha\right)T = c_1\end{aligned}. \tag{23}$$

Then, the resulting equation will be solved by integration using MATHEMATICA software:

$$\begin{aligned}F = {} & \frac{E_2}{R_2{}^2(r-2R_2) - \nu R_2{}^2(r-2R_2+1)}e^{\zeta\left(\frac{r}{R_2}-1\right)}\\ & \times\left[\frac{rEi\frac{r}{R_2} - R_2 e^{\frac{r}{R_2}}}{E_2 e} - \left(-\beta_\alpha R_2^2 e^{\zeta\left(1-\frac{r}{R_2}\right)}(r+2R_2)\right.\right.\\ & \left.+\eta_\alpha\frac{r^2}{2}\right)T - \left(-\beta_\alpha R_2 e^{\zeta\left(1-\frac{r}{R_2}\right)}(r+2R_2) + \eta_\alpha\frac{r^2}{2}\right)T\\ & \left.+\frac{r^2}{2}C_1 + rC_3 + C_4\right].\end{aligned} \tag{24}$$

where C_3 and C_4 are the constants of integration

By substituting Eq. (24) into Eqs. (15) and (16) to obtain the radial and tangential stresses,

the radial stress, tangential stress, and radial displacement are expressed as follows:

$$\begin{aligned}\sigma_r = {} & \frac{E_2}{R_2{}^2(r-2R_2) - \nu R_2{}^2(r-2R_2+1)}e^{\zeta\left(\frac{r}{R_2}-1\right)}\\ & \times\left[\frac{Ei\frac{r}{R_2} - R_2 e^{\frac{r}{R_2}}}{rE_2 e} - \left(-\beta_\alpha R_2^2 e^{\zeta\left(1-\frac{r}{R_2}\right)}\left(1+\frac{2R_2}{r}\right)\right.\right.\\ & \left.+\eta_\alpha\frac{r}{2}\right)T - \left(-\beta_\alpha R_2 e^{\zeta\left(1-\frac{r}{R_2}\right)}\left(1+\frac{2R_2}{r}\right) + \eta_\alpha\frac{r}{2}\right)T + \frac{r}{2}C_1\\ & \left.+C_3 + \frac{1}{r}C_4\right].\end{aligned} \tag{25}$$

$$\begin{aligned}\sigma_\theta = &-\frac{R_2^2 e^{\zeta\left(\frac{r}{R_2}-1\right)} Ei\left(\frac{r}{R_2}\right) e'(R_2^2(r-2R_2)-\nu R_2^2(r-2R_2+1))}{re(R_2^2(r-2R_2)-\nu R_2^2(r-2R_2+1))^2} + \frac{\nu R_2^2 e^{\zeta\left(\frac{r}{R_2}-1\right)} Ei\left(\frac{r}{R_2}\right) e'(R_2^2(r-2R_2)-\nu R_2^2(r-2R_2+1))}{re(R_2^2(r-2R_2)-\nu R_2^2(r-2R_2+1))^2}\\ &- \frac{\nu R_2^3 e^{\zeta\left(\frac{r}{R_2}-1\right)} e'(R_2^2(r-2R_2)-\nu R_2^2(r-2R_2+1))}{re(R_2^2(r-2R_2)-\nu R_2^2(r-2R_2+1))^2} + \frac{R_2^3 e^{\zeta\left(\frac{r}{R_2}-1\right)} e'(R_2^2(r-2R_2)-\nu R_2^2(r-2R_2+1))}{re(R_2^2(r-2R_2)-\nu R_2^2(r-2R_2+1))^2}\\ &+ \frac{R_2 e^{\frac{2r}{R_2-1}} - e^{\zeta\left(\frac{r}{R_2}-1\right)} Ei\left(\frac{r}{R_2}\right)}{r^2 e(R_2^2(r-2R_2)-\nu R_2^2(r-2R_2+1))} + \frac{(1-r)e^{\frac{2r}{R_2-1}}}{r^2 e(R_2^2(r-2R_2)-\nu R_2^2(r-2R_2+1))}\\ &+ 2E_2\frac{\beta_\alpha R_2^2(2R_2+1)(R_2^2-\nu R_2^2)}{(R_2^2(r-2R_2)-\nu R_2^2(r-2R_2+1))^2}T + 2E_2\left(-\frac{\gamma_\alpha e^{\zeta\left(\frac{r}{R_2}-1\right)}}{2(R_2^2(r-2R_2)-\nu R_2^2(r-2R_2+1))}\right.\\ &\left.- \frac{\gamma_\alpha e^{\zeta\left(\frac{r}{R_2}-1\right)}}{2R_2(R_2^2(r-2R_2)-\nu R_2^2(r-2R_2+1))} + \frac{\gamma_\alpha r(R_2^2-\nu R_2^2)e^{\zeta\left(\frac{r}{R_2}-1\right)}}{2(R_2^2(r-2R_2)-\nu R_2^2(r-2R_2+1))^2}\right)T\\ &+ \frac{E_2 e^{\zeta\left(\frac{r}{R_2}-1\right)}(r-1)(R_2^2(r-2R_2)-\nu R_2^2(r-2R_2+1))C_1}{2R_2(R_2^2(r-2R_2)-\nu R_2^2(r-2R_2+1))^2}\\ &- \frac{E_2 e^{\zeta\left(\frac{r}{R_2}-1\right)}((R_2^2-\nu R_2^2)+(R_2^2(r-2R_2)-\nu R_2^2(r-2R_2+1)))C_1}{2R_2(R_2^2(r-2R_2)-\nu R_2^2(r-2R_2+1))^2}\\ &+ \frac{E_2 e^{\zeta\left(\frac{r}{R_2}-1\right)}((R_2^2(r-2R_2)-\nu R_2^2(r-2R_2+1))-R_2(R_2^2-\nu R_2^2))C_3}{R_2(R_2^2(r-2R_2)-\nu R_2^2(r-2R_2+1))^2}\\ &+ \frac{E_2 e^{\zeta\left(\frac{r}{R_2}-1\right)}(r(R_2^2(r-2R_2)-\nu R_2^2(r-2R_2+1))-rR_2(R_2^2-\nu R_2^2))C_4}{r^2R_2(R_2^2(r-2R_2)-\nu R_2^2(r-2R_2+1))^2}\\ &- \frac{E_2 e^{\zeta\left(\frac{r}{R_2}-1\right)}R_2(R_2^2(r-2R_2)-\nu R_2^2(r-2R_2+1))C_4}{r^2R_2(R_2^2(r-2R_2)-\nu R_2^2(r-2R_2+1))^2}.\end{aligned} \tag{26}$$

$$\begin{aligned}\delta = &\frac{E_2R_2(r-R_2)E_2}{R_2^2(r-2R_2)-\nu R_2^2(r-2R_2+1)}e^{2\zeta\left(\frac{r}{R_2}-1\right)}\times\left[\frac{rEi\frac{r}{R_2}-R_2e^{\frac{r}{R_2}}}{rE_2e} - \left(-\beta_\alpha R_2^2 e^{\zeta\left(1-\frac{r}{R_2}\right)}(r+2R_2)+\eta_\alpha\frac{r^2}{2}\right)T\right.\\ &\left.- \left(-\beta_\alpha R_2 e^{\zeta\left(1-\frac{r}{R_2}\right)}(r+2R_2)+\eta_\alpha\frac{r^2}{2}\right)T + \frac{r^2}{2}C_1 + rC_3 + C_4\right] - \nu R_2 e^{\zeta\left(\frac{r}{R_2}-1\right)} + R_2(r+2R_2)\beta_\alpha e^{\zeta\left(\frac{r}{R_2}-1\right)}T + \frac{r^2}{2}\eta_\alpha T - \frac{r^2}{2}C_1\\ &- r\cos\theta C_2 = 0,\end{aligned} \tag{27}$$

where

$$C_1 = \frac{4R_2^2}{r^2}(r+2R_2)\beta_\alpha e^{\zeta\left(1-\frac{r}{R_2}\right)}T + 3\eta_\alpha T - \frac{2\nu}{r^2}R_2e^{\zeta\left(\frac{r}{R_2}-1\right)} + \frac{2R_2}{r^2}\beta_\alpha e^{\zeta\left(\frac{r}{R_2}-1\right)}T, \tag{28}$$

$$C_2 = 0, \tag{29}$$

$$\begin{aligned}C_3 = &-\frac{Ei\frac{r}{R_2}-R_2e^{\frac{r}{R_2}}}{rE_2e} + \left(-\beta_\alpha R_2^2 e^{\zeta\left(1-\frac{r}{R_2}\right)}\left(1+\frac{2R_2}{r}\right)+\eta_\alpha\frac{r}{2}\right)T + \left(-\beta_\alpha R_2 e^{\zeta\left(1-\frac{r}{R_2}\right)}\left(1+\frac{2R_2}{r}\right)+\eta_\alpha\frac{r}{2}\right)T\\ &- \left(\frac{2R_2^2}{r}(r+2R_2)\beta_\alpha e^{\zeta\left(1-\frac{r}{R_2}\right)} + \frac{3r}{2}\eta_\alpha\right)T + \frac{\nu}{r}R_2e^{\zeta\left(\frac{r}{R_2}-1\right)} + \frac{R_2}{r}\beta_\alpha e^{\zeta\left(\frac{r}{R_2}-1\right)}T,\end{aligned} \tag{30}$$

$$C_4 = 0. \tag{31}$$

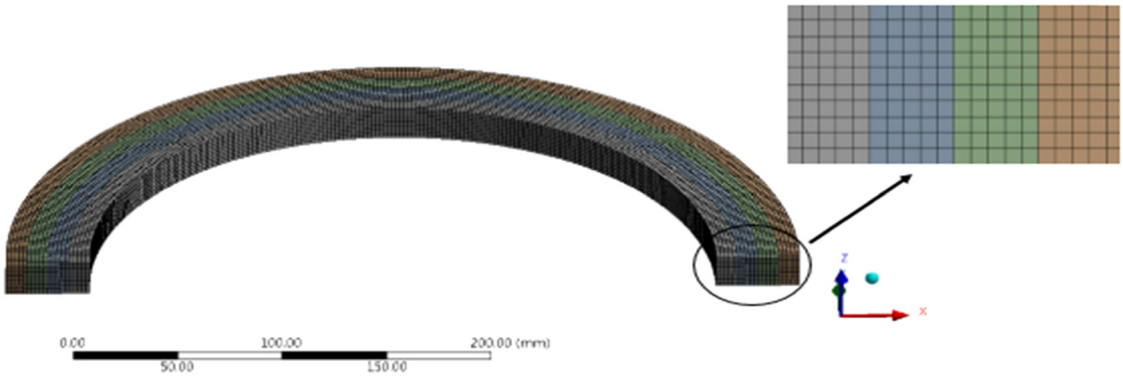

Figure 2: Mesh details of the FGM curved beam model.

Thus, the equivalent stress (von Mises stress) is determined using Eqs. (26) and (27) as follows:

$$\sigma_{\mathrm{e}} = \sqrt{\sigma_{\mathrm{r}}^2 - \sigma_{\mathrm{r}}\sigma_{\theta} + \sigma_{\theta}^2}. \tag{32}$$

2.4 Temperature variation distributions

The exponential function indicates how the temperature distribution varies through the curved beam as a function of r. So, T_1 is the temperature acting on the FGM curved beam's inner

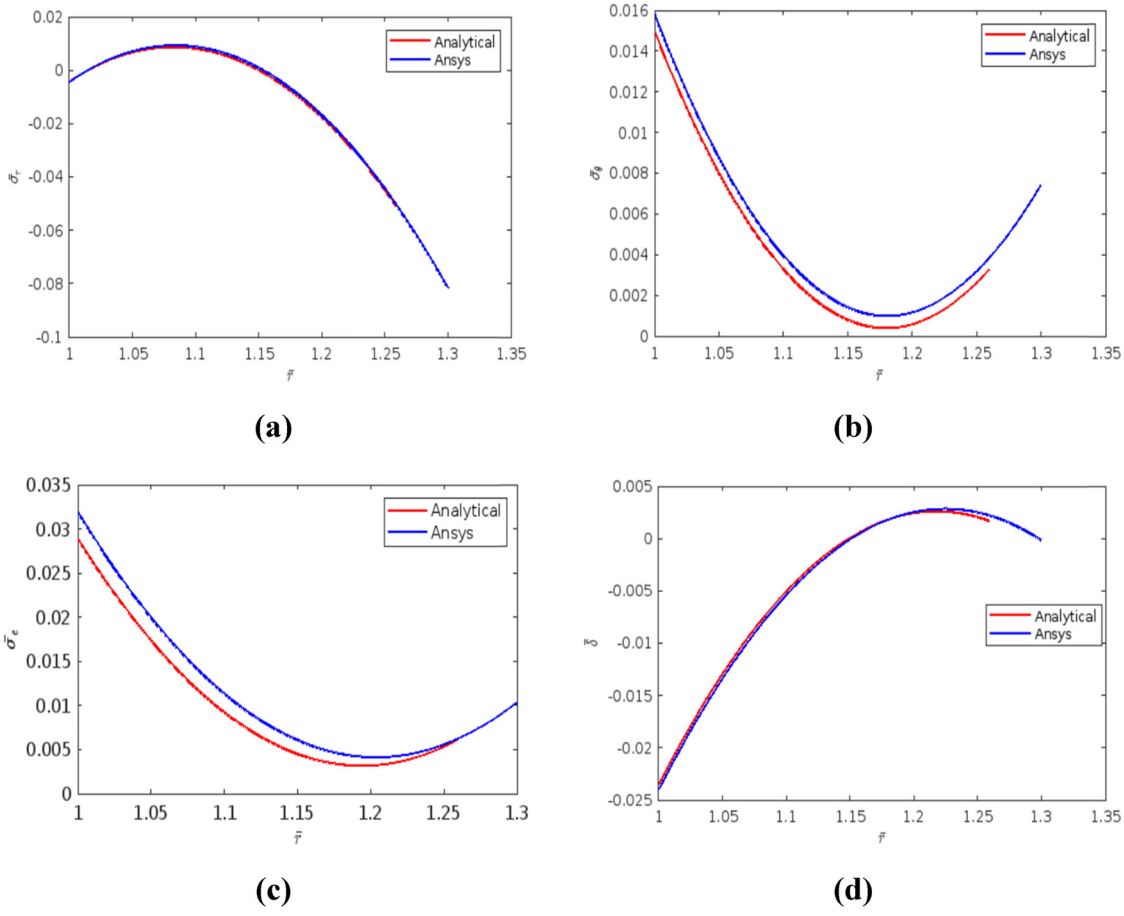

Figure 3: Variation of (a) radial stress $\bar{\sigma}_{\mathrm{r}}$, (b) tangential stress $\bar{\sigma}_{\theta}$, (c) equivalent stress (von Mises) $\bar{\sigma}_{\mathrm{e}}$, and (d) deformation $\bar{\delta}$ through the radius $\bar{r}$ of aluminum steel FGM curved beam at ambient temperature $\bar{T} = 0.2112$, $\bar{E}_2 = 0.345$, $\nu = 0.33$, and $\zeta = 5.53$.

surface, and T_2 is the temperature acting on its outer surface. The one-dimensional heat conduction is as follows [28]:

$$\frac{1}{r}\frac{\mathrm{d}}{\mathrm{d}r}\left[rk(r)\frac{\mathrm{d}T(r)}{\mathrm{d}r}\right] = 0, \tag{33}$$

$$\frac{1}{r}\frac{\mathrm{d}}{\mathrm{d}r}\left[r\left(\beta_\alpha \mathrm{e}^{\zeta\left(1-\frac{r}{R_2}\right)} + \eta_\alpha\right)\frac{\mathrm{d}T(r)}{\mathrm{d}r}\right] = 0. \tag{34}$$

By integration

$$T(r) = -\frac{K_1}{\beta_\alpha e\left(Ei\left(-\frac{r}{R_2}\right) + R_2\mathrm{e}^{-\frac{r}{R_2}}\right) - \eta_\alpha \ln(r)} + K_2, \tag{35}$$

where Ei is an exponential function and K_1 and K_2 are the constants of integration

$$\begin{cases} \Delta T = T_2 - T_1 \\ T = T_1 \text{ on } r = R_1. \\ T = T_2 \text{ on } r = R_2 \end{cases} \tag{36}$$

3 Results and discussions

Based on the previous analytical analysis, a thermo-elastic solution is derived by conducting stress calculations for a rectangular curved beam made of FGM with varying parameters. A curved beam with a radius of the inner surface of 150 mm and a radius of the outer surface of 190 mm is considered for the derived analysis. The curved beam's inner and outer materials are considered to be pure steel, with $E_1 = 200 \times 10^3$ MPs and aluminum with $E_2 = 69 \times 10^3$ MPs, respectively, and $\nu = 0.3$. Thus, a 3D curved beam model is created using Ansys software to verify the analytical solution. The FGM curved beam model is created using a double couple of mechanical and thermal structures in Ansys Workbench. The model consists of four layers, with each layer measuring 5 mm in thickness. The element size conducted for the mesh is 2 mm, as shown in Figure 2. The model consists of 265,508 nodes and 53,600 elements across all layers. The boundary conditions

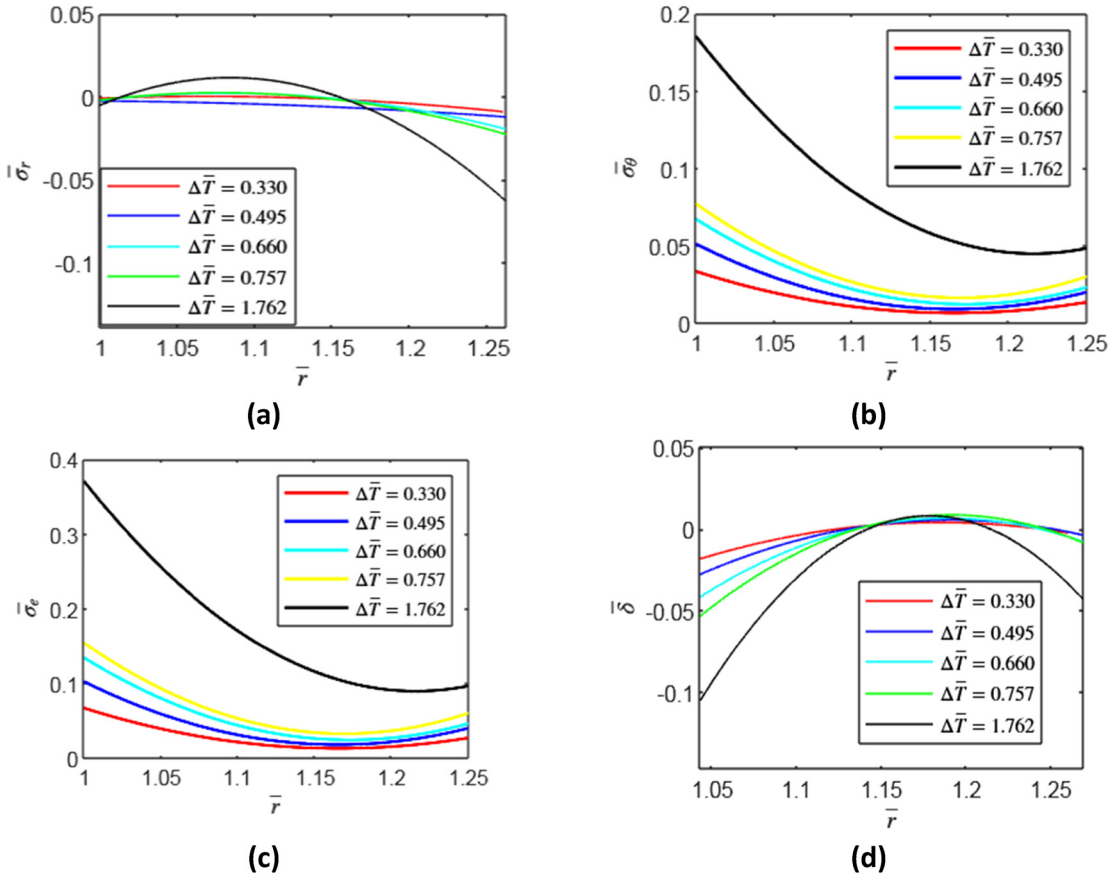

Figure 4: Variation of (a) radial stress $\bar{\sigma}_r$, (b) tangential stress $\bar{\sigma}_\theta$, (c) equivalent stress (von Misses) stress $\bar{\sigma}_e$, (d) deformation $\bar{\delta}$ through the radius $\bar{r}$ of aluminum steel FGM curved beam with different temperature range and grading constants ($\nu = 0.33$, $\beta_\alpha = -5.7 \times 10^{-6}$, $\eta_\alpha = -5.4 \times 10^{-5}$, $\zeta = 5.53$).

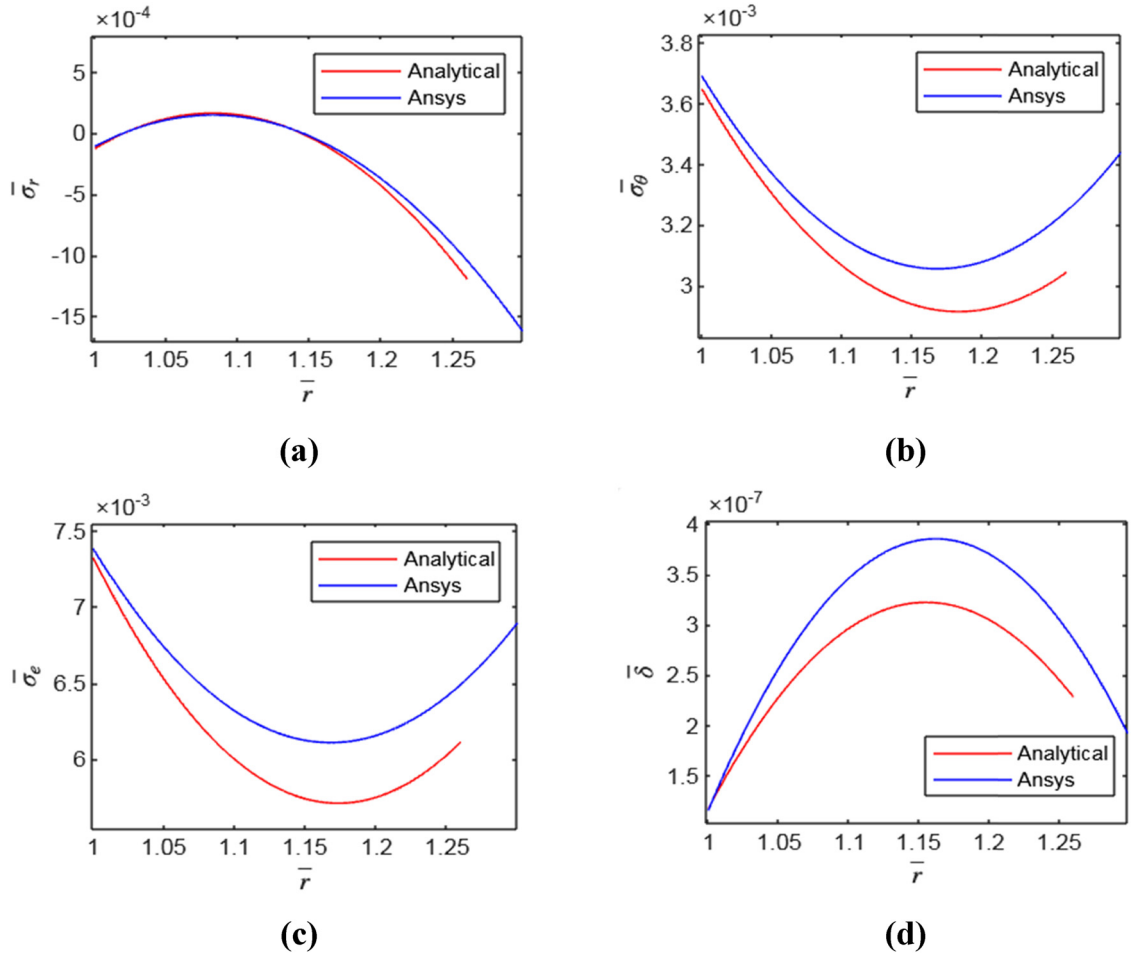

Figure 5: Variation of (a) radial stress $\bar{\sigma}_r$, (b) tangential stress $\bar{\sigma}_\theta$, (c) equivalent stress (von Misses) $\bar{\sigma}_e$, and (d) deformation $\bar{\delta}$ through the radius $\bar{r}$ of Ti-6Al-4v/ZrO FGM cured beam at ambient temperature $\bar{T} = 0.0248$, $\bar{E}_2 = 0.2968$, $\nu = 0.3$, and $\zeta = 0.24$.

considered are double bending moments (M = 100 N. M) acting at the two ends of the FGM curved beam at the ambient temperature, which is considered 22°C.

The following normalized values are introduced as follows:

$$\bar{E} = \frac{E(r)}{E_1}, \quad \bar{\rho} = \frac{\rho(r)}{\rho_1}, \bar{\alpha} = \frac{\alpha(r)}{\alpha_1}, \quad \bar{r} = \frac{r}{R_1}, \quad \bar{T} = \frac{\alpha_1(r)E_1(r)T(r)}{\sigma_{y_1}}, \tag{37}$$

$$\bar{\sigma}_r = \frac{\sigma_r}{\sigma_{y_1}}, \bar{\sigma}_\theta = \frac{\sigma_\theta}{\sigma_{y_1}}, \bar{\sigma}_e = \frac{\sigma_e}{\sigma_{y_1}}, \bar{\delta} = \frac{\delta}{R_1}. \tag{38}$$

The analytical radial, tangential, and equivalent stresses and deformations are conducted as normalized quantities and compared with the Ansys software, as shown in Figure 3. The normalized stresses and deformations were obtained from $\bar{r} = 1$ (inner surface) across the thickness line with $\bar{r} = 1.06, 1.13, 1.20$ and finally 1.25, which represent the outer surface of FGM curved beam.Thus, the error between the FEA and analytical results for radial, tangential, and von Mises stress and deformation does not exceed 0.06%, with good agreement for the radial, tangential, and equivalent (von Mises) stresses and deformation.

It is probable that the FGM curved beam's mechanical properties, incorporating its modulus of elasticity, coefficient of thermal expansion, density, and applied temperature, vary with its radius. Thus, using Eqs. (25)–(27), and (32), the stress distribution is calculated according to Equation (38), and the variation of temperature values is conducted as described in the study by Haskul [28]. Figure 4 shows the variation of the normalized stresses and deformation through the ratio of r/R_1, which represents the curved beam's radius. Stress variation was conducted with a variation in the temperature surface $\Delta\bar{T}$, $\bar{T}_1 = 0$, and the considered grading parameters are $\beta_\alpha = -5.7 \times 10^{-6}$, $\eta_\alpha = -5.4 \times 10^{-5}$, and $\zeta = 5.53$.

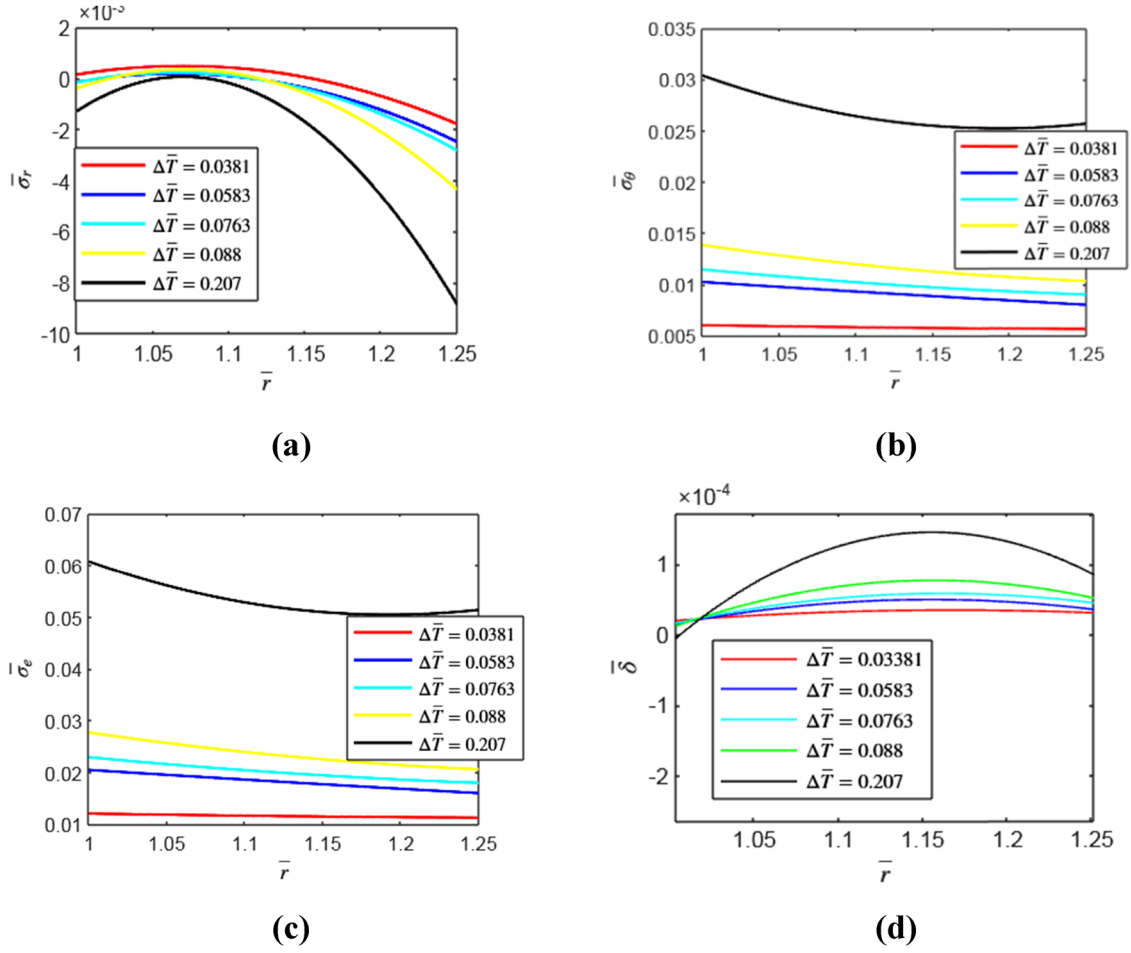

Figure 6: Variation of (a) radial stress $\bar{\sigma}_r$, (b) tangential stress $\bar{\sigma}_\theta$, (c) equivalent stress (von Misses) stress $\bar{\sigma}_e$, and (d) deformation $\bar{\delta}$ through the radius $\bar{r}$ of Ti-6Al-4v/ZrO_2 FGM curved beam with different temperature ranges and grading constants (ν = 0.3, $\beta_\infty = -1.041 \times 10^{-5}$, $\eta_\alpha = 2.355 \times 10^{-6}$, ζ = 0.24).

The radial stress at the curved beam's inner surface is close to zero and negative values and then increases slightly along the normalized curved beam's radius between $\bar{r}$ = 1.05 and $\bar{r}$ = 1.17 with increases in the surface temperature difference. Then, the radial stress decreases with an increase in the surface temperature difference, as shown in Figure 4(a). The tangential stresses recorded the highest values at the curved beam's inner surface $\bar{r}$ = 1 for the difference in surface temperature $\Delta\bar{T}$ = 1.729, and through the beam radius $\bar{r}$, the tangential stress decreases with a decrease in the temperature difference, as shown in Figure 4(b). Thus, the von Mises stresses recorded the highest values at $\Delta\bar{T}$ = 1.729 and decreased with a decrease in temperature difference, as shown in Figure 4(c). Figure 4(d), illustrates the variation of deformations along the curved beam's normalized radius; the highest deformation values are recorded at $\Delta\bar{T}$ = 0.330, Also, deformation rises across the curved beam's radius and reduces as the temperature differential grows. The plotted graphs illustrate the calculated stresses and deformation at $\bar{r}$ = 1.25, which represent 98% aluminum and 2% steel, which is consistent with the mixture law.

3.1 Impact of different FGMs curved beams

In this section, another material of the FGM curved beam is considered to enhance the effect of grading parameters in the results. The assumed material in this case investigation is Ti-6Al-4V/ZrO_2, which is used in several applications, including high-performance automobile parts, aerospace fasteners, aircraft structural components, and biomedical applications. Furthermore, the material considered for the inner surface of the curved beam is Ti-6Al-4V with $E_1 = 122.56 \times 10^3$ MPa, ν = 0.29, $\alpha_1 = 7.579 \times 10^{-6}$1/°C and ZrO_2 Zirconia for the outer surface of the curved beam

$E_2 = 116.4 \times 10^3$ MPa, $\nu = 0.3$, $\alpha_1 = 8.7 \times 10^{-6}$1/°C [29]. Thus, the considered grading parameters are $\beta_\alpha = -1.041 \times 10^{-5}$, $\eta_\alpha = 2.355 \times 10^{-6}$, $\zeta = 0.24$. The results obtained for the FGM material considered under the same boundary conditions show that there is a significant difference in the values of the stresses and deformation. So, this led to the fact that the material indices have a noticeable effect on the results. Figure 5 compares the analytical and FEA results for mechanical stresses and deformation, showing good agreement; the error percentage does not exceed 0.9%. Moreover, radial, tangential, and equivalent stresses and deformation are plotted as normalized quantities. The plotted graphs illustrate the calculated stresses and deformation at $\bar{r} = 1.25$, which represents 98% Ti-6Al-4V and 2% ZrO_2, which is consistent with the mixture law.

Figure 6 illustrates the variation of normalized thermal stresses and deformation along the radius of the curved beam with variations in the temperature difference across the surface. The stress and deformation values are less than those of a steel/aluminum curved beam. Consequently, grading parameters significantly impact the behavior of stress and deformation.

4 Conclusion

An analytical solution is presented for a thermo-elastic model of a rectangular curved beam composed of FGM, considering exponential material grading in the radial direction. Timoshenko beam theory is utilized to generate the governing equations. The study examines the effect of radial material gradation on stress and deformation behavior under combined mechanical and thermal loading. The total stresses and deformations are analyzed for two FGM curved beams: an aluminum/steel FGM beam and a Ti-6Al-4V/ZrO_2 FGM beam. Parametric studies reveal the following key conclusions regarding the effects of exponential grading parameters and temperature variations:

- The exponential grading parameters have a significant influence on the stresses and deformations of the FGM curved beam. The results show that normalized radial stresses are nearly zero at the inner surface of the curved beam and decrease as the steady-state temperature increases.
- Normalized tangential and equivalent stresses increase with rising steady-state temperatures.
- Normalized deformation decreases with decreasing steady-state temperature along the radial direction.
- The stresses and deformation in the Ti-6Al-4V/Zro_2 FGM beams are lower than those in the aluminum/steel FGM beam due to the higher strength and stiffness of Ti-6Al-4V/Zro_2. Reduced deformation is achieved by combining the durability and strength of Ti-6Al-4V with the high hardness and elastic modulus of zirconia.
- The analytical results are validated against FEA (ANSYS), with normalized stresses and deformations plotted using MATLAB.

Funding information: The authors state no funding involved.

Author contributions: All authors have accepted responsibility for the entire content of this manuscript and approved its submission.

Conflict of interest: The authors state no conflict of interest.

References

[1] Pandey PM, Rathee S, Srivastava M, Jain P. Functionally graded material (FGMs) fabrications, properties, applications and advancements. Boca Raton: CRC Press; 2022.
[2] Miyamoto Y, Kaysser WA, Rabin BH, Kawasaki A, Ford RG. Functionally graded materials design, processing and applications. New York: Kluwer Acadmic Publisher; 1999.
[3] Maalawi K. Optimization of functionally graded material structures: Some case studies. In Optimum Composite Structures. London: IntechOpen; 2019. p. 158–91.
[4] Pavlović G, Savković M, Zdravković N, Marković G, Gašić M. Optimization of crane hooks considered as curved beams with different cross-sections – a comparative study using MATLAB. Hoisting and conveying equipment and technologies. In *International Conference MHCL*, Belgrade, 2019.
[5] Pei YL, Li LX. A simplified theory of FG curved beams. Eur J Mech/A Solids. 2021;85:1–10.
[6] He XT, Li X, Li WM, Sun JY. Bending analysis of functionally graded curved beams with different properties in tension and compression. Arch Appl Mech. 2019;89:1973–94.
[7] Pydah A, Sabale A. Static analysis of bi-directional functionally graded curved beams. Composite Struct. 2016;160:867–76.
[8] Avhad PV, Sayyad AS. Static analysis of functionally graded composite beams curved in elevation using higher order shear and normal deformation theory. ScienceDirect. 2020;21:1195–9.
[9] Zhang P, Qing H, Gao CF. Exact solutions for bending of Timoshenko curved nanobeams made of functionally graded materials based on stress-driven nonlocal integral model. Compos Struct. 2020;245:112362.
[10] Belarbi MO, Garg A, Houari MS, Hirane H, Tounsi A, Chalak HD. A three unknown reined shear beam element model for buckling analysis of functionally graded curved sandwich beams. Eng Comput. 2021;38:4273–300.
[11] Karamanli A, Wattanasakulpong N, Nazargah ML, Vo TP. Bending, buckling and free vibration behaviours of 2D functionally graded curved beams. Structures. 2023;55:778–98.

[12] Nikrad FS, Kanellopoulos A, Bodaghi M, Chen TZ. Large deformation behavior of functionally graded porous curved beams in thermal environment. Arch Appl Mech. 2021;91:2255–78.
[13] Hu YJ, Zhou H, Zhu W, Zhu J. A thermally-coupled elastic large-deformation model of a multilayered functionally graded material curved beam. Compos Struct. 2020;244:1–14.
[14] Tang Y, Tang F, Zheng J, Li Z. In-plane asymmetric buckling of an FGM circular arch subjected to thermal and pressure fields. Eng Struct. 2021;239:1–16.
[15] Wan ZQ, Li SR, Ma HW. Geometrically nonlinear analysis of functionally graded Timoshenko curved beams with variable curvatures. Adv Mater Sci Eng. 2019;2019:1–10.
[16] Allam MN, Radwan AF. Nonlocal strain gradient theory for bending, buckling, and vibration of viscoelastic functionally graded curved nanobeam embedded in an elastic medium. Adv Mech Eng. 2019;11(4):1–15.
[17] Beg MS, Yasin MY. Bending, free and forced vibration of functionally graded deep curved beams in thermal environment using an efficient layerwise theory. Mech Mater. 2021;159:1–15.
[18] Pandey S, Pradyumna S. Thermal shock response of porous functionally graded sandwich curved beam using a new layerwise theory. Mech Based Des Struct Mach. 2021;51(4):2055–79.
[19] Liang Y, Zheng S, Wang H, Chen D. Nonlinear isogeometric analysis of axially functionally graded graphene platelet reinforced composite curved beams. Compos Struct. 2024;330:117871.1–117871.13.
[20] Tornabene F, Viscoti M, Dimitri R. Effect of thermal and electric coupling on the multifield response of laminated shell structures employing higher-order theories. Compos Struct. 2025;354:1–36.
[21] Brischetto S, Carrera E. Thermal stress analysis by refined multilayered composite shell theories. J Therm Stresses. 2008;32:165–86.
[22] Shirdelan F, Mohammadimehr M, Bargozini F. Control and vibration analyses of a sandwich doubly curved micro-composite shell with honeycomb, truss, and corrugated cores based on the fourth-order shear deformation theory. Appl Math Mech. 2024;45(10):1773–90.
[23] Civalek O, Baltacıoglu AK. Free vibration analysis of laminated and FGM composite annular sector plates. Compos Part B. 2019;157:182–94.
[24] Mahajan VM, Sharma A. Evaluation of static responses for layered composite arches. Curved Layer Struct. 2023;10:1–14.
[25] Hussein AA, Jabbar NA, Ahmed SS, Aljibori HS, Mohammed MN, Alturaihi MH, et al. Study of heat transfer through functionally graded material fins using analytical and numerical investigations. Curved Layer Struct. 2025;12:1–13.
[26] Habib E-S, Mahdy AI, Ali G, El-Megharbel A, El-Shrief E. Analysis of a thick cylindrical FGM pressure vessel with variable parameters using thermoelasticity. Curved Layer Struct. 2023;10(1):1–13.
[27] Timoshenko SP, Goodier JN. Two dimensional problem in polar coordinates. In Theory of elasticity. New York: Mc Graw-Hill Book Company; 1970.
[28] Haskul M. Elastic state of functionally graded curved beam on the plane stress state subject to thermal load. Mech Based Des Struct Mach. 2019;48(6):739–54.
[29] Boga C, Seleek O. Stress analysis of functionally graded beams due to thermal loading. J Eng Sci Technol. 2020;15(1):55–65.